34. FACIES AND DIAGENESIS OF ORGANIC MATTER IN NANKAI TROUGH SEDIMENTS, DEEP SEA DRILLING PROJECT LEG 87A[1]

P. K. Mukhopadhyay, J. Rullkötter, R. G. Schaefer, and D. H. Welte, Institut für Erdöl und Organische Geochemie[2]

ABSTRACT

A series of upper Pliocene to Pleistocene sediment samples from DSDP Sites 582 and 583 (Nankai Trough, active margin off Japan) were investigated by organic geochemical methods including organic carbon determination, Rock-Eval pyrolysis, gas chromatography of extractable hydrocarbons, and kerogen microscopy. The organic carbon content is fairly uniform and moderately low (0.35 to 0.77%) at both sites, although accompanied by high sedimentation rates. The low organic matter concentrations are the result of the combined effect of several factors: low bioproductivity, oxic depositional environment, and dilution with lithogenic material. Organic petrography revealed a mixture of three maceral types: (1) fresh, green fluorescent alginites of aquatic origin probably transported by turbidites from the shelf edge, (2) gelified huminites and particulate liptinites derived from the erosion of unconsolidated peat, and (3) highly reflecting inertinites derived from continental erosion. By a combination of organic petrography and Rock-Eval pyrolysis results, the organic matter is characterized as mainly type III kerogen with a slight tendency to a mixed type II-III. During Rock-Eval pyrolysis, a mineral matrix effect on the generated hydrocarbons was observed. The organic matter in all sediments has a low level of maturity (below 0.45% R_m) and has not yet reached the onset of thermal hydrocarbon generation according to several geochemical maturation parameters. This low maturity is in contrast to anomalously high extract yields at both sites and large hydrocarbon proportions in the extracts at Site 583. This contrast may be due to early generation of polar compounds and perhaps redistribution of hydrocarbons caused by subduction tectonics.

Carbon isotope data of the interstitial hydrocarbon gases indicate their origin from bacterial degradation of organic matter, although only very few bacterially degraded maceral components were detected.

INTRODUCTION

The Nankai Trough (Fig. 1) is part of a slowly subsiding trench and the major active margin off Japan. Two sites were drilled during Leg 87A. Site 582 is located on the floor of the Nankai Trough about 2 km south of the deformation front. The sediments at this site are mainly dark olive gray turbidites and hemipelagic clays, silts, and sands filling the trench axis (Leg 87 Scientific Party, 1983). From Holes 582 and 582B undeformed upper Pliocene to Quaternary sediments were recovered. Hole 582B penetrated approximately 560 m of trench-fill sediments overlying a lower Quaternary and upper Pliocene hemipelagic section, similar in appearance to Shikoku Basin sediments, to a total depth of 749.4 m. The approximate age of the base of the trench-fill strata is 0.65 Ma. Drilling at Site 583 was performed in the stratigraphically equivalent but deformed sediments of the basal thrust sheets underlying the landward slope (Karig et al., 1983). The sediments at this "zone of accretion" are lower to upper Quaternary and consist of dark olive gray turbidites, graded turbidites, and hemipelagic clays, with thin and frequent graded sand and silt layers interrupted by sparse layers of ash and vitric sands. At both sites the carbonate content is very low because of deposition below the calcite compensation depth (CCD). There are, however, rare thin carbonate-rich layers of crystalline pale yellow aggregates.

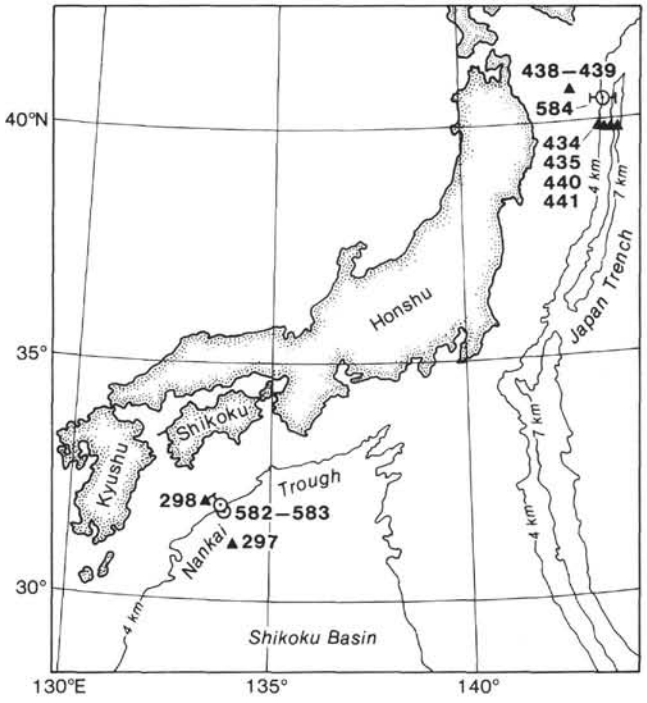

Figure 1. Location map of the Nankai Trough and Japan Trench (Leg 87A) indicating the earlier and present drill sites off Japan.

Our primary objective was to study the nature of both the soluble and insoluble fractions of the organic matter and its diagenetic evolution, including a comparison be-

[1] Kagami, H., Karig, D. E., Coulbourn, W. T., et al., *Init. Repts. DSDP*, 87: Washington (U.S. Govt. Printing Office).

[2] Addresses: (Mukhopadhyay, present address) Bureau of Economic Geology, University of Texas at Austin, Austin, Texas 78713; (Rullkötter, Schaefer, and Welte) Institut für Erdöl und Organische Geochemie (ICH-5), P.O. Box 1913, Kernforschungsanlage Jülich GmbH, D-5170 Jülich 1, Federal Republic of Germany.

tween the deformed and undeformed sediments, the former supposedly affected by subduction.

The sediments also contained high levels of gaseous hydrocarbons and nonhydrocarbons. One of the objectives of Leg 87A was to drill into a gas hydrate zone, whose presence had been indicated by a bottom simulating seismic reflector. This goal was abandoned for safety reasons during drilling, but the high gas concentrations suggest the presence of such a gas hydrate zone. A short compositional and isotopic study of the gases has been added to the organic matter analysis.

METHODS

Frozen samples were thawed and then dried at 50°C for 12 hours and ground; some unground subsamples were saved for microscopic observation. Total organic carbon was determined with the LECO IR-112 carbon analyzer after treatment of the sediments with HCl to remove the carbonate carbon. Bitumen fractions were obtained using a modified flow-blending extraction technique (Radke et al., 1978) and dichloromethane as solvent. Fractionation of the total extracts into saturates, aromatics, and N, S, O-compounds plus residue was performed by automated medium pressure liquid chromatography (Radke et al., 1980).

The capillary gas chromatograms of the nonaromatic hydrocarbon fractions were obtained using a Siemens L 350 gas chromatograph that was equipped with a glass capillary column (25 m long, with an inner diameter of 0.3 mm) coated with SE 54 silicone elastomer as the stationary phase. Helium was used as the carrier gas, and the oven was programmed for the following temperatures: 80°C initial temperature (hold for 2 minutes), 3°C/minute heating rate, and 270°C final temperature. The hydrocarbon fractions were dissolved in *n*-heptane, and the split ratio was 1:10. Normalized C_{15}-C_{36} *n*-alkane distributions (sum of peak areas equals 100%), carbon preference indices (CPI values), and isoprenoid hydrocarbon concentration ratios are based on peak area integration using a Kratos-Instem Datachrom II system.

Rock-Eval pyrolysis was performed according to the method described by Espitalié and others (1977). Hydrogen and oxygen contents of the rock samples, measured as hydrocarbon compound and carbon dioxide yields, respectively, were normalized to organic carbon and displayed as index values in a diagram adopted from Espitalié and others (1977) and Peters and Simoneit (1982). In order to assess the mineral matrix effect on hydrocarbon compound generation during Rock-Eval pyrolysis (Espitalié et al., 1980), five pure kerogen samples have also been studied.

The kerogen concentration procedure for microscopy included treatment with 4N HCl followed by flotation in a density solution (ZnI_2, 1.9 g/cm^3). For Rock-Eval pyrolysis, kerogens were separated after treatment with 4N HCl and 40% HF followed by density separation. Maceral composition analysis was carried out using transmitted, normal, and fluorescence-reflected light microscopy. For details of the instrumentation for maceral analysis and vitrinite reflectance measurements as well as the nomenclature of the maceral types, see Gormly and Mukhopadhyay (1983) and Stach and others (1982). Huminite/vitrinite and other maceral particles measured are grains larger than 10 μm in diameter.

RESULTS AND DISCUSSION

Organic Carbon

Figure 2 and Table 1 show the organic carbon content of 47 sediments and 5 kerogen samples from both sites. Organic carbon values of the Site 582 sediments vary between 0.55 and 0.73% down to a depth of 500 m, irrespective of sediment lithology and nature. In other words, there is no difference between the hemipelagic muds and the turbiditic sandy clays. Beyond 500 m the organic carbon is lower than 0.5%, although the difference is not very large. This change more or less coincides with the boundary between the trench-fill sediments and the

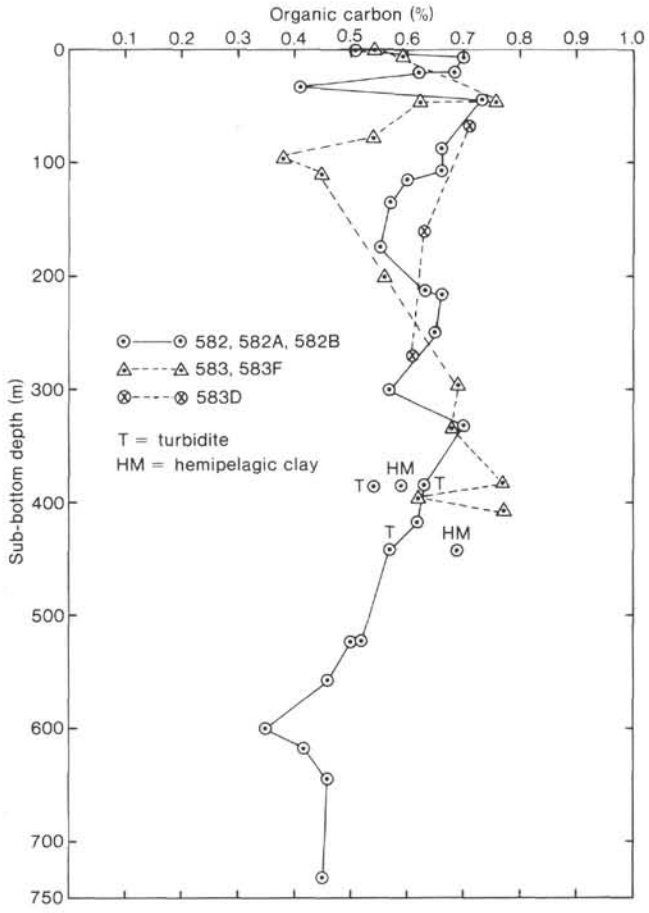

Figure 2. Plot of the organic carbon content (% dry weight) against depth (m) from Sites 582 and 583.

hemipelagites related to the Shikoku Basin section (site chapter, Site 582, this volume; Leg 87 Scientific Party, 1983). At Site 583, we analyzed the organic carbon content in sediments from four holes (583, 583F, 583B, and 583D). In Holes 583 and 583F the variation ranges between 0.38 and 0.77%. The lowest values are observed around 100 m depth, whereas the shallower and deeper samples contain more than 0.5% C_{org} (Fig. 2). In Hole 583B we measured only one sample, which contains abundant visible plant fragments and therefore shows a high organic carbon content (6.99%) (sample not included in Fig. 2). From Hole 583D, three sediment samples were measured with C_{org} values between 0.61 and 0.71%. Organic carbon distribution is generally similar at Sites 582 and 583 (Fig. 2). The organic carbon content of the separated kerogen varies between 63.8 and 87.69% (Table 1). A high carbon content in an immature kerogen generally indicates the presence of inertinite (Stach et al., 1982).

Compared with typical pelagic deep-sea sediments, which usually contain less than 0.2% C_{org}, the organic carbon contents at Sites 582 and 583 are significantly elevated. This indicates that organic matter accumulation here is influenced by downslope transport processes such as slumping or turbidite flow. Relative to other turbidite sequences with high sediment accumulation rates (300 to 900 m/Ma), the organic carbon contents at Sites 582

Table 1. Lithology, stratigraphy, organic carbon content, and Rock-Eval pyrolysis data for samples from Sites 582 and 583.

Hole-Core-Section (interval in cm)	Sub-bottom depth (m)	Stratigraphy	Lithology	Organic carbon (%)	Rock-Eval pyrolysis: Hydrogen index (mg HC/g C_{org})	Rock-Eval pyrolysis: Oxygen index (mg CO_2/g C_{org})	Rock-Eval pyrolysis: Production index $\frac{S_1}{S_1 + S_2}$	Rock-Eval pyrolysis: T_{max} (°C)
Nankai Trough floor								
582-1-1, 74-76[a]	0.75		Olive gray mud	0.51	53	250	0.28	414
582-1-5, 70-72	6.70		Same as above	0.70	68	397	0.25	550
582-3-6, 70-71[a]	23.10		Dark gray sandy mud	0.68	80	507	0.21	412
582-3-6, 133-139	23.40		Same as above with deformed structures	0.62[b] 69.72[c]	59 137	689 115	0.20 0.16	416 419
582A-1-3, 70-70[a]	32.80		Gray sandy mud	0.41	59	447	0.24	385
582A-2-3, 70-75[a]	42.50		Very dark gray sandy mud	0.73	74	602	0.23	420
582B-5-1, 110-112[a]	88.40		Gray mud	0.66	68	509	0.22	419
582B-7-1, 36-39[a]	106.87		Gray mud	0.66	88	649	0.22	420
582B-7-6, 11-24	114.20		Gray mud	0.60	63	728	0.19	415
582B-10-1, 29-31[a]	135.60		Whitish gray mud	0.57	62	657	0.22	417
582B-14-1, 18-20[a]	174.20		Gray mud	0.55	70	641	0.21	414
582B-18-1, 27-41	212.85		Silty mud with cracks	0.63	65	699	0.19	416
582B-18-4, 16-19[a]	217.18		Same as above	0.66	107	575	0.25	412
582B-22-1, 69-72[a]	251.80	Quaternary	Gray mud (HM)	0.65	71	766	0.22	413
582B-29-2, 15-30	300.80		Sandy volcanic mud (HM)	0.57	52	644	0.18	417
582B-30-3, 135-137[a]	332.26		Dark gray mud (HM)	0.70	100	803	0.25	414
582B-36-1, 95-96[a]	385.75		Olive gray mud (HM)	0.59	93	387	0.24	411
582B-36-1, 102-103[a]	385.82		Gray mud with mottles (T)	0.63	67	708	0.24	418
582B-36-1, 116-117[a]	385.94		Gray mud with mottles (T)	0.54	70	716	0.20	423
582B-39-3, 91-105	416.68		Gray sandy mud with cracks	0.62	57	509	0.17	415
582B-42-2, 10-12[a]	443.11		Same as above (T)	0.57	74	567	0.21	422
582B-42-5, 85-87[a]	443.87		Gray mud (nannofossil rich) (HM)	0.69	74	471	0.20	417
582B-50-4, 40-54	523.26		Gray mudstone	0.52	42	440	0.17	417
582B-50-6, 80-81[a]	526.10		Same as above (T)	0.50	70	381	0.22	429
582B-54-1, 72[a]	557.22		Muddy silt (T)	0.46	51	436	0.23	418
582B-58-5, 40-42[a]	601.31		Sandy gray mud (T)	0.35	62	394	0.31	350
582B-60-2, 108-124	616.76		Green mudstone (silty)	0.42	35	409	0.20	352
582B-63-2, 80-82[a]	645.21		Olive gray mudstone	0.46	67	397	0.31	353
582B-72-1, 61-71	731.66	upper Pliocene	Dark greenish gray mudstone	0.45	45	483	0.17	402
Zone of accretion								
583-1-1, 74-76	0.75	upper Quaternary	Biosiliceous sandy mud (HM)	0.54	48	393	0.23	404
583-2-5, 8-25	11.66	upper Quaternary	Biosiliceous sandy mud (HM)	0.59[b] 71.88[c]	59 181	223 86	0.23 0.10	386 443
583-7-2, 5-7[a]	46.46	middle Quaternary	Dark gray mud (HM)	0.76	721	640	0.26	410
583-7-2, 123-137	47.70	middle Quaternary	Gray mud (HM)	0.62[b] 63.80[c]	57 167	671 120	0.19 0.14	407 430
583-11-3, 0-2[a]	76.51	middle Quaternary	Sandy mud	0.54	62	406	0.27	408
583-14-1, 5-7[a]	92.06	upper-lower Quaternary	Sandy mud	0.38	56	512	0.21	404
583-17-2, 40-54	108.97	upper-lower Quaternary	Silty mud with sand	0.45[b] 74.09[c]	42 19	514	0.17 0.38	393
583F-6-2, 82-96	201.10	lower Quaternary	Gray mud with sand	0.56	49	547	0.17	424
583F-12-1, 54-55[a]	256.84	lower Quaternary	Chondrites bearing mud (HM)	0.64	55	294	0.28	407
583F-16-1, 63-77	295.70		Biscuited gray mud (HM)	0.69	45	429	0.15	422
583F-20-2, 1-3[a]	335.12		Silty mud	0.68	76	636	0.20	423
583F-25-1, 80-82[a]	382.61	lower Quaternary	Firm gray mud (HM)	0.77	182	472	0.14	422
583F-26-3, 25-39	394.82		Dark gray mud	0.62[b] 70.52[c]	45 150	429 75	0.15 0.13	422 431
583F-29-2, 14-16[a]	422.05		Silty mud	0.77	120	554	0.23	431
Zone of accretion, thrust toe								
583B-1-3, 27-30[a]	3.28	upper Quaternary	Gray volcanogenic mud with plant fragments	6.99	126	234	0.25	338
583D-3-1, 92-106	67.00	upper Quaternary	Gray nannofossil mud	0.71	62	669	0.22	399
583D-13-1, 100-114	163.37	middle Quaternary	Biosiliceous silty mud (HM)	0.63	46	613	0.16	423
583D-24-1, 100-114	269.77	middle Quaternary	Biscuited olive gray mud	0.61[b] 87.69[c]	54 103	594 38	0.17 0.15	422 445

Note: HM = hemipelagic mud; T = turbidite.
[a] Samples taken during shipboard study.
[b] Whole rock.
[c] Kerogen concentrate.

and 583 are still fairly low and strikingly uniform. This may be caused by the combined effects of low autochthonous bioproductivity, deposition in a deep oxic environment, and dilution by an abundance of lithogenic material.

Rock-Eval Pyrolysis

For each sample studied, Table 1 gives the hydrogen index (mg HC/g C_{org}), oxygen index (mg CO_2/g C_{org}), production index,[3] and temperature of maximum pyrolysis yield (T_{max}, °C). Plotted on a Van Krevelen-type diagram (Espitalié et al., 1977; Tissot et al., 1979), most samples fall outside the range because of high oxygen index values (Fig. 3). This distribution is very common for deep-sea sediments (Peters and Simoneit, 1982). Rock-Eval pyrolysis of the Nankai Trough sediments suggests

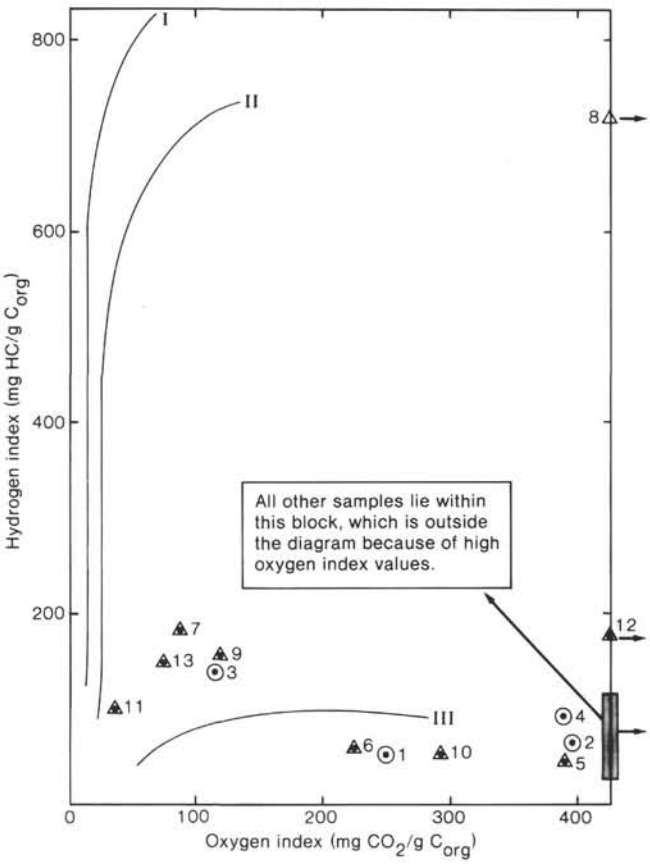

Figure 3. Results of Rock-Eval pyrolysis displayed as hydrogen index values for Sites 582 and 583. Roman numerals correspond to kerogen types. Arabic numbers indicate samples as follows: 1 = 582-1-1, 74–76 cm; 2 = 582-1-5, 70–72 cm; 3 = 582-3-6, 133–139 cm (kerogen); 4 = 582B-36-1, 95–96 cm; 5 = 583-1-1, 74–76 cm; 6 = 583-2-5, 8–25 cm; 7 = 583-2-5, 8–25 cm (kerogen); 8 = 583-7-2, 5–7 cm; 9 = 583-7-2, 123–137 cm (kerogen); 10 = 583F-12-1, 54–56 cm; 11 = 583D-24-1, 110–114 cm (kerogen); 12 = 583F-25-1, 80–82 cm; 13 = 583F-26-3, 25–39 cm (kerogen).

[3] Production index $= \frac{\text{mg free hydrocarbons already generated or migrated into the sediment}}{\text{mg free hydrocarbons + mg hydrocarbons produced during pyrolysis.}}$

This definition is also expressed as $\frac{S_1}{S_1 + S_2}$.

that they mostly contain oxygen-rich type III or IV kerogen. The hydrogen index value of Sample 583-7-2, 5–7 cm, which is plotted in the top right of Figure 3, appears to be erroneous.

In contrast to most of these data, the higher hydrogen index values for all five separated kerogens indicate a mixed kerogen type II-III. This discrepancy of hydrogen index values between untreated and demineralized samples suggests a mineral matrix effect during pyrolysis of the untreated sediments. As suggested by Espitalié and others (1980) and Gormly and Mukhopadhyay (1983), hydrocarbon retention during pyrolysis increases with the clay content of rocks, especially in rocks with a low organic carbon content. In those rocks a major portion of the heavy hydrocarbons liberated during pyrolysis is retained by the mineral matrix. In the Nankai Trough sediments, the mineral matrix effect accounts for an increase of the hydrogen index by a factor of two to three in the isolated kerogens. The decrease of the oxygen index values at the same time may be due to the hydrolysis of oxygen-bearing functional groups during the strong acid treatment (Müller, pers. commun., 1983). Taking both effects into account, we tend to classify the kerogens of most Nankai Trough sediments as type III or type II-III (close to type III).

Maceral Composition

The nature of the organic matter can also be revealed from the maceral composition (Table 2). Apart from Sample 582-3-6, 133–139 cm, kerogens in the remaining 18 samples contain more than 80–90% macerals from a terrestrial source; these include huminite/vitrinite, inertinite, sporinite, cutinite, and resinite or suberinite. As an exception, a significant amount of fresh large alginite particles (mostly thalloid; more than 60–80μm) accounts for 19% of total macerals in Sample 582-3-6, 133–139 cm. At Site 582, the sediments frequently contain nonoxidized framboidal pyrite in small quantities. In contrast to our earlier studies of the sediments from the Japan Trench and the Shikoku Basin (Rullkötter, Cornford, et al., 1980; Rullkötter, Flekken, et al., 1980), recycled vitrinite populations (more than 1% mean vitrinite reflectance, $\overline{R}_m$) in Nankai Trough sediments are not very abundant. Huminites (for brown coal petrography nomenclature of vitrinites below 0.5% $\overline{R}_m$, see Stach et al., 1982) are mainly eu-ulminite and gelinite, whereas at Site 583 eu-ulminite, textinite, and phlobaphinites are mixed. In Sample 583-1-1, 74–76 cm, yellow fluorescent textinite with an excellently preserved woody structure was observed. The difference in the nature of huminite macerals and the proportion of alginite between Samples 582-3-6, 133–139 cm and 583-1-1, 74–76 cm suggest a slight difference in early diagenesis between these two sites. Some of the huminite/vitrinite grains show Newton rings on their surface. After solvent extraction, this impregnation persists, which suggests a very strong impregnation with migrated or early diagenetic hydrocarbons/nonhydrocarbons on the vitrinite surface. Apart from this impregnating soluble bitumen, solid bitumen (granular dark gray in normal reflected light and yellowish brown in fluorescent reflected light) was found in

Table 2. Maceral composition, huminite/vitrinite reflectance, and sclerotinite reflectance data for samples from Sites 582 and 583.

Hole-Core-Section (interval in cm)	Sub-bottom depth (m)	Organic carbon (%)	Huminite reflectance $\bar{R}_m$ (mean)	Huminite reflectance Standard deviation	Minimum reflectance of sclerotinite or semifusinite grain (%)	Organic facies (vol.% of maceral composition) 1	2	3	4	5	6	7	8
582-1-5, 70–72	6.70	0.70	0.17	0.06	0.26	50	35		9	2	4		
582-3-6, 133–139	23.40	0.62	0.19	0.03	0.28	52	20		5	4	19		
582B-7-6, 11–24	114.20	0.60	0.20	0.04	0.28	69	15		8		7		
582B-18-1, 27–41	212.85	0.63	0.21	0.06	0.27	62	18		12	2	6		
582B-29-2, 15–30	300.80	0.57	0.23	0.04	0.27	48	29	1	13	3	6		
582B-39-3, 91–105	416.68	0.62	0.26	0.03	0.35	43	29		21	3	4		
582B-50-4, 40–54	523.26	0.52	0.29	0.06	0.35	49	30		12	2	3		
582B-60-2, 108–124	616.76	0.42	0.32	0.08	0.43	52	22		11 (mainly resinite & cutinite)		4	2	9
582B-72-1, 61–71	731.66	0.45	0.40	0.07	0.56	40	26	3	16 (mainly resinite)	4	9		2
583-1-1, 74–76	0.75	0.54	0.20	0.06	0.27	35	30	2	18	6	9		
583-2-5, 8–25	11.66	0.59	0.20	0.04	0.27	48	30	1	3	4	7	4	
583-7-2, 123–137	47.70	0.62	0.20	0.04	0.28	58	29		8	1	4		
583-17-2, 40–54	108.97	0.45	0.23	0.03	0.32	52	30		6	1	11		
583F-6-2, 82–96	201.10	0.56	0.24	0.07	0.38	58	30		10				2
583F-16-1, 63–77	295.66	0.69	0.25	0.06	0.40	40	42		4	5	8		1
583F-26-3, 25–39	394.82	0.62	0.28	0.07	0.46	50	25		12		10		3
583D-3-1, 92–106	67.00	0.71	0.19	0.04	0.28	29	50	2	11	1	7		
583D-13-1, 100–114	163.37	0.63	0.25	0.06	0.39	58	25		5	4	8		
583D-24-1, 100–114	269.77	0.61	0.26	0.05	0.40	50	22		18 (3% resinite)	4	6		

Note: 1 = huminite/vitrinite; 2 = inertinite; 3 = amorphous humic matter (humosapropelinite); 4 = particulate liptinite B (sporinite-cutinite-suberinite-resinite); 5 = particulate liptinite A (phytoclasts and zooclasts); 6 = alginite; 7 = amorphous liptinite (sapropelinite I and II); 8 = solid bitumen.

some samples, for example, in Sample 582B-60-2, 108–127 cm (9%).

The sediments at Site 583 contain some bimacerite or trimacerite grains (vitrinite, suberinite/resinite with or without inertodetrinite; Sample 583-7-2, 123–137 cm) that are absent at Site 582. At Site 582, recycled vitrinites or vitrinites of unknown origin (no evidence of recycling, specifically oxidation or corrosion) having higher reflectance values above 1% occur mainly below 400 m depth. At both sites the huminites/vitrinites having reflectance values up to 0.8% are the main maceral components. Recycled spores (brown fluorescent) are not common except in Samples 582B-72-1, 61–71 cm; 583-1-1, 74–76 cm; and 583D-24-1, 100–114 cm. In these samples both green and brown/red fluorescent sporinites occur together.

Among the autochthonous terrestrial higher plant liptinites, suberinite, resinite, and few pollens are common in most of the kerogen samples. Samples 583-1-1, 74–76 cm and 582B-60-2, 108–124 cm contain some resinites whose inner cores are yellow and whose outer parts have a brown fluorescent color suggesting transportation or weathering.

Apart from the fresh, green fluorescent thalloid alginites in phytoclasts and zooclasts, fragments of acritarchs and fish (red fluorescent) are common (582-3-6, 133–139 cm). Biodegraded liptinitic and humic matter are almost absent from the Nankai Trough sediments. Only in Sample 583-2-5, 8–25 cm does some yellowish brown fluorescent amorphous liptinite mass (sapropelinite II, Mukhopadhyay et al., 1985; bituminite I or II, of Teichmüller and Ottenjann, 1977) with remnants of dinoflagellates occur. A few gray, amorphous, and granular macerals (with very dark brown fluorescence) are observed in some samples (582B-72-1, 61–71 cm; 583-1-1, 74–76 cm; 583-2-5, 8–25 cm; 583D-3-1, 92–106 cm). Their presence can be attributed to humosapropelinite (Mukhopadhyay et al., 1985; or bituminite III of Teichmüller and Ottenjann, 1977), which is supposed to be the biodegradation product of humic material.

The inertinite content in the Nankai Trough sediments does not show a definite relationship to depth or location. Inertinites are mostly sclerotinite or inertodetrinite. Most of the sclerotinite has low reflectance values ($\bar{R}_m$ between 0.28–0.54%). Semi-fusinite with incipient cell structure is rare. Some sediments (e.g., 582B-72-1, 61–71 cm) contain micrinitized phytoclasts (acritarchs?). No true pyrofusinite, macrinite, or degradofusinite were observed. In general, the inertinite content in these sediments exceeds 20%.

Comparing both maceral composition and Rock-Eval pyrolysis (considering the mineral-matrix effect and hydrolysis of oxygen-containing compounds during acid treatment), we can best classify the kerogens (as before) as type III and type II-III (close to type III). The type II-III kerogens are mixtures of vitrinite/inertinite and alginite in generally vitrinite-rich sediments.

Origin of Organic Matter and Transport Processes

From the organic petrographic data it is obvious that the kerogens contain mixtures of three types of macerals: (1) textinite, eu-ulminite, gelinite associated with sub-

erinite, resinite, pollen, and low-reflectance sclerotinite, all from a swamplike environment where Eh/pH conditions are suitable for biochemical gelification; (2) thalloid algae from a subaquatic environment; and (3) residual kerogen-like, high-reflectance vitrinites, inertodetrinite, semifusinite, inertinitized phytoclasts, and bimacerite grains, indicating erosion of coal or matured kerogen-containing landmass. Therefore, it is assumed that the Nankai Trough sediments are fed by three organic matter sources: subaerial reducing, subaquatic, and subaerial oxidizing. Moreover, fresh ulminite and gelinite together with fresh algae indicate a very active biochemical gelification process in one of the source areas and rapid short distance transportation by debris flow or through fecal pellets. The provenance of the organic matter types (1) and (2) suggests a combination of near source and rapid transportation, although from a different facies, and that of type (3) indicates a distal source transportation. Sedimentologists for Leg 87A (see site chapter, Site 582, this volume) suggest that turbidites are fed to the Nankai Trough from the Tokai drainage basin off central Japan, a distance of about 400 km. We assume that a major part of the residual organic matter may be transported like this but a near-source admixture is also evident.

Extractable Organic Matter

In contrast to the fairly uniform composition of the total organic carbon, the extractable organic material is highly variable in gross composition (Table 3). At Site 582, N, S, O compounds are the major components (more than 95%) in the sediment extracts below 25 m depth and there is very little fluctuation. Two samples (582-3-6, 133–139 cm; 582B-60-2, 108–124 cm) show anomalously high extract yields (561 and 490 ppm). Extract yields at this site vary between 53 and 561 ppm. For comparison, the yield at Site 583 lies between 70 and 473 ppm. The sediments from Holes 583 and 583F contain higher hydrocarbon concentrations than those from Holes 583D, 582, and 582B. Similar to Site 582, sediments in the upper 25 m at Site 583 contain more hydrocarbons than those beneath (at Hole 583D the change is at 67 m depth). There is a relationship between high extract yield, N, S, O compounds/residue, and solid bitumen content by microscopy. Compared to other young deep-sea sediments (Rullkötter, Mukhopadhyay, and Welte, 1984), the production index from Rock-Eval pyrolysis is anomalously high in all Nankai Trough sediments. A plot of the extract yield versus the production index shows a good relationship for these two parameters for the Site 582 sediments but no such relationship at Site 583 (Fig. 4).

Nonaromatic Hydrocarbons

The capillary gas chromatograms of the nonaromatic hydrocarbon fractions revealed very uniform compositions, particularly in terms of their *n*-alkane distributions (Fig. 5) for most of the samples studied from Sites 582 and 583. Most of the distributions have the following features in common:

1. strong relative abundance of *n*-alkanes in the higher molecular weight range ($\geq C_{27}$);
2. *n*-alkane envelope curve peaking at C_{29} or C_{31}; and
3. high predominance of odd-numbered *n*-alkanes over their even-numbered homologs in the higher molecular weight range. Accordingly, carbon preference indices reach values up to 5.2 for CPI_{29} (Table 4).

Exceptions to these features were found, in particular, in Sample 582-3-6, 133-139 cm (possibly because of some algal contribution).

The *n*-alkanes are the dominant peaks in the gas chromatograms of the nonaromatic hydrocarbon fractions (Figs. 6B, 6C, 6D and 7B, 7C, 7D). Only traces of branched or cyclic compounds other than pristane and phytane and a major contaminant (diisobutylphthalate) eluting between *n*-nonadecane (C_{19}) and *n*-eicosane (C_{20}) can be seen. However, some samples reveal nonaromatic hydrocarbon compositions that are different. Samples 582-3-6, 133–139 cm (Fig. 6A); 582B-72-1, 61–71 cm (Fig. 6E); 583-1-1, 74–76 cm (mudline contamination?); and 583-17-2, 40–54 cm show bimodal *n*-alkane distri-

Table 3. Extract (bitumen) and liquid chromatography yields for samples from Sites 582 and 583.

Hole-Core-Section (interval in cm)	Sub-bottom depth (m)	Organic carbon (%)	Extract (ppm)	Extract (mg/g C_{org})	C_{15+} hydrocarbons (mg/g C_{org})	C_{15+} saturated hydrocarbons (% of extract)	C_{15+} aromatic hydrocarbons (% of extract)	N,S,O compounds and residue (% of extract)
582-1-5, 70–72	6.70	0.70	119	17.0	3.4	8.0	12.0	80.0
582-3-6, 133–139	23.40	0.62	561	90.5	16.8	12.0	6.6	81.4
582B-7-6, 11–24	114.20	0.60	351	58.5	1.7	2.8	0.1	97.1
582B-18-1, 27–41	212.85	0.63	250	39.7	1.7	2.9	1.4	95.7
582B-29-2, 15–30	300.80	0.57	262	46.0	3.0	4.6	1.9	93.5
582B-39-3, 91–105	416.68	0.62	361	58.2	1.3	1.3	1.0	97.7
582B-50-4, 40–54	523.26	0.52	130	25.0	1.0	0.8	3.3	95.9
582B-60-2, 108–124	616.76	0.42	490	116.7	2.8	0.1	2.3	97.6
582B-72-1, 61–71	731.66	0.45	53	11.8	0.8	6.5	0.1	93.4
583-1-1, 74–76	0.75	0.54	300	55.6	30.8	25.9	29.6	44.5
583-2-5, 8–25	11.66	0.59	261	44.2	27.7	38.1	24.6	37.3
583-7-2, 123–137	47.70	0.62	158	25.5	6.0	4.7	18.7	76.6
583-17-2, 40–54	108.97	0.45	473	105.1	10.0	2.8	6.7	90.5
583F-6-2, 82–96	201.10	0.56	196	35.0	8.1	5.9	17.1	77.0
583F-16-1, 63–77	295.66	0.69	70	10.1	4.1	12.3	27.7	60.0
583F-26-3, 25–39	394.82	0.62	148	23.9	6.9	6.7	22.2	71.1
583D-3-1, 92–106	67.00	0.71	109	15.4	8.1	20.5	32.5	47.0
583D-13-1, 100–114	163.37	0.63	354	56.2	6.0	2.3	8.3	89.4
583D-24-1, 100–114	269.77	0.61	264	43.3	6.5	3.0	12.0	85.0

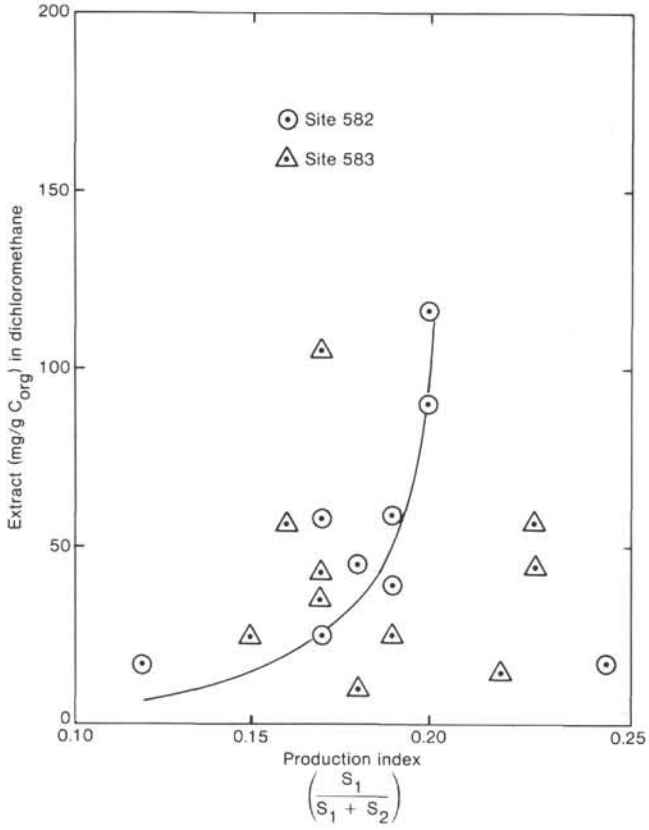

Figure 4. Plot of the extract yield versus production index in Rock-Eval pyrolysis. Line is best visual fit for Site 582 samples only. For explanation of production index, see Rock-Eval Pyrolysis section.

butions with one maximum between C_{17} and C_{19} and a second at C_{29} or C_{31}. The first maximum is supposed to be due to either (shipboard) contamination or the presence of eroded, more mature organic matter, whereas the second maximum represents terrestrial higher plant waxes as in the other samples. Sample 583-2-5, 8–25 cm has a pronounced, chromatographically unresolved hump in the C_{25} molecular range (Fig. 7A). This may reflect intense bacterial reworking of originally terrigenous organic material.

Pristane and phytane are minor components in all samples, and the pristane/phytane concentration ratio is significantly above 1.

The *n*-alkane distributions of most of the samples from Sites 582 and 583 compare well with those of a comprehensive series of Pleistocene/Neogene samples from the Japan Trench (Rullkötter, Cornford, et al., 1980), also showing the dominance of terrigenous wax alkanes.

Maturation

Most kerogens at both sites in the Nankai Trough contain very broad huminite/vitrinite populations (Figs. 8 and 9), but the range between 0.1 and 0.8% $\overline{R}_m$ is dominant in most cases. Table 2 gives the mean values and standard deviations for all huminite/vitrinite reflectance data. Similar to the multimodal vitrinite populations, sclerotinite (a maceral within the inertinite group) also

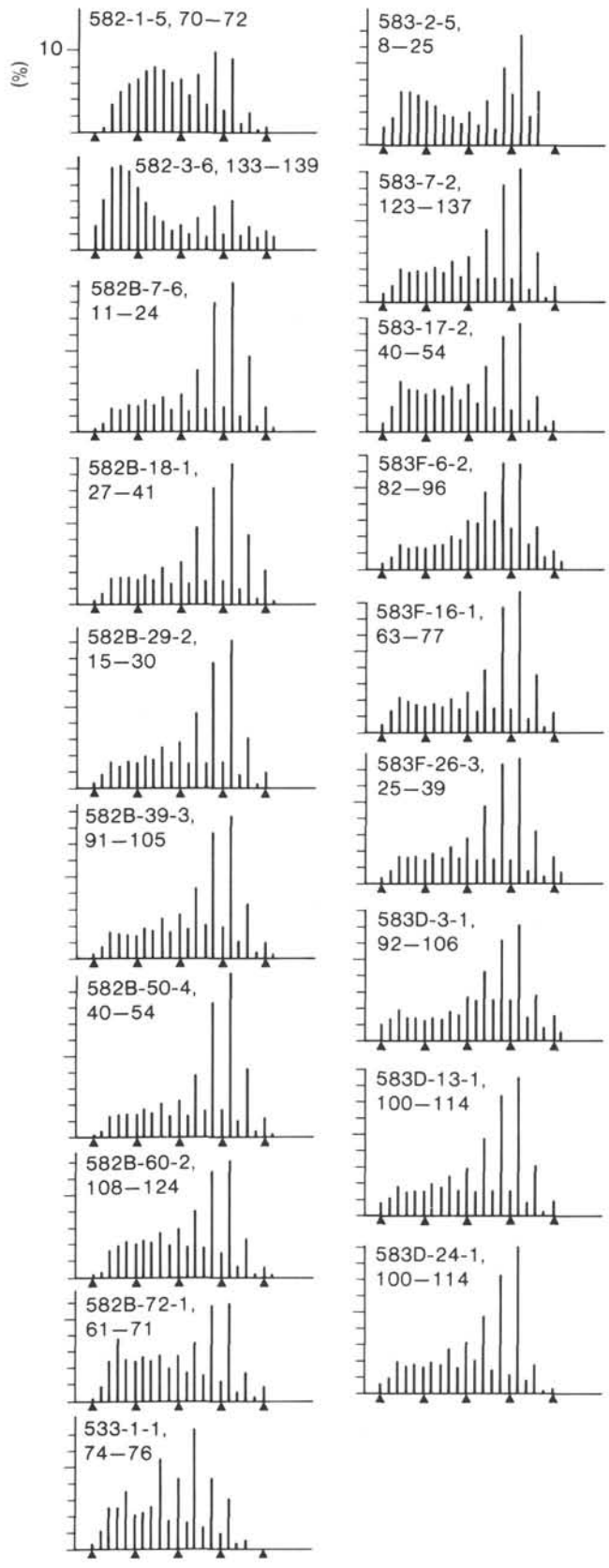

Figure 5. *n*-alkane distribution (sum of peak areas = 100%) for Leg 87A sediment samples. Triangles indicate C_{15}, C_{20}, C_{25}, C_{30}, and C_{35} *n*-alkanes, plotted from left to right.

Table 4. Carbon preference indices (CPI) and isoprenoid hydrocarbon ratios for Leg 87A sediment samples.

Hole-Core-Section (interval in cm)	CPI_{25-31}	CPI_{29}	CPI_{27-29}	Pristane/ *n*-heptadecane	Phytane/ *n*-octadecane	Pristane/ phytane
582-1-5, 70–72	2.32	3.19	2.41	0.88	0.55	1.07
582-3-6, 133–139	2.33	2.84	2.48	0.61	0.46	1.31
582B-7-6, 11–24	4.15	5.19	4.02	0.89	0.53	1.77
582B-18-1, 27–41	4.26	4.79	4.09	0.96	0.54	1.92
582B-29-2, 15–30	4.16	4.96	3.99	1.39	0.67	2.21
582B-39-3, 91–105	3.31	3.93	3.10	1.10	0.69	1.67
582B-50-4, 40–54	4.00	4.84	3.72	1.04	0.56	1.69
582B-60-2, 108–124	2.96	3.60	2.80	0.93	0.49	1.53
582B-72-1, 61–71	3.01	3.93	2.96	0.86	0.33	1.63
583-1-1, 74–76	3.68	3.52	4.18	0.71	2.15	0.24
583-2-5, 8–25	2.29	2.23	2.27	0.75	0.72	1.03
583-7-2, 123–137	4.06	4.91	3.95	0.99	0.55	1.97
583-17-2, 40–54	3.29	4.08	3.21	0.99	0.56	2.10
583F-6-2, 82–96	2.03	2.32	1.96	1.31	0.96	1.58
583F-16-1, 63–77	4.14	5.14	3.94	1.09	0.67	1.84
583F-26-3, 25–39	3.95	4.83	3.98	1.38	0.73	1.83
583D-3-1, 92–106	2.22	2.42	2.06	0.79	0.57	1.72
583D-13-1, 100–114	4.02	4.70	3.89	1.17	0.57	2.43
583D-24-1, 100–114	4.23	5.12	4.02	1.11	0.71	1.78

shows variable reflectance values. Because sclerotinite is an inertinite maceral, the lowest reflectance of sclerotinite in a sediment should be higher than the highest reflectance of autochthonous huminite particles in the same sediment, if it is not bitumen-impregnated. Because most of the sediments (except a few samples) contain very few bimacerite grains with vitrinite or recycled vitrinite grains showing features of weathering or oxidation (i.e., oxidation rims, corroded grains, etc.), we used the minimum sclerotinite reflectance as a parameter for deciphering the upper boundary of the autochthonous huminite/vitrinite populations (Figs. 8 and 9). In some samples, the boundary was determined from vitrinite in a bimacerite or trimacerite grain (e.g., in Sample 583-1-1, 74–76 cm) or from semifusinite reflectance (582B-72-1, 61–71 cm). In transmitted light, the thermal alteration index of greenish yellow pollen (TAI 1^+) and brownish yellow pollen (TAI 2^+ or 3) provides further evidence for a mixed origin of the terrigenous organic matter particles and allows a further assessment of the maturity level of the unaltered (autochthonous) organic matter.

The measured mean huminite (autochthonous) reflectance values range from 0.17 to 0.40% at Site 582 (down to a depth of 731.4 m) and from 0.19 to 0.28% at Site 583 (maximum depth 394.82 m). The mean huminite reflectance values show an increase with depth in spite of the low maturation level (Figs. 8 and 9). At Site 582, recycled vitrinites or vitrinite of unknown origin (no evidence of recycling) with reflectance values above 1% $\overline{R}_m$ occur mainly below 400 m depth.

The temperature measured at Site 582 was 28.8°C at a sub-bottom depth of 508 m with a temperature gradient of 4.38 ± 0.15°C/100 m, which should give a temperature of about 40°C at 750 m depth. Compared to similar Pliocene-Pleistocene sediments (Dow, 1978; Bostick et al., 1979) with an absolute temperature of 40°C, our measured value of 0.4% R_m is somewhat high. The cause of this high reflectance may be that the thermal conductivity of some of the Nankai Trough sediments is high (Yamano, 1982) or that the measured huminite grains are from an already semiconsolidated peat surface.

The temperature of maximum pyrolysis yield (Table 1) does not show a gradient with depth at Site 582, but there may be an increase with depth at Site 583 (from 400 to 422°C; equivalent vitrinite reflectance values are 0.3 and 0.45% according to Teichmüller and Durand, 1983). These calculated vitrinite reflectance values are higher than the measured ones, probably because pyrolysis also includes recycled organic matter, whereas a selection of the primary particles was made during reflectance measurements.

The high carbon preference indices (CPI 2–4) of the *n*-alkanes in both wells indicate immaturity of all sediments and agree with the vitrinite reflectance data. In general, there is no relation between CPI and sediment depth.

Composition of the Gases

Hydrocarbon and nonhydrocarbon gases, mainly methane (up to a volume of 85%) with very minor C_2, C_3, iC_4, isopentane and neopentane, minor CO_2, and traces of H_2S are present as gas pockets down to a depth of 601 m at Site 582. No solid gas hydrates were encountered at either site. In Hole 583F the relative amount of methane increased to 94% at 400 m sub-bottom (site chapter, Site 583, this volume).

The isotopic compositions ($\delta^{13}C$ and δD) of the methane of five samples from Sections 583-2-5 (12 m), 583F-12-1 (256.5 m), 583F-18-3 (318 m), 583F-24-1 (372.5 m), and 583F-27-1 (401.5 m) were determined. The $\delta^{13}C$ values vary between −73.5 and −66.83‰. The δD values vary between −187.7 and −191.5‰.

The isotopic composition (Schoell, 1982; 1983) and the high methane content and ubiquitous presence of CO_2 indicate that the gas originated from bacterial degradation of organic matter. The nature and isotopic composition of the Nankai Trough gases and the amount and type of the organic matter are very similar to Pliocene-Pleistocene gases and organic matter from the Italian Po Basin (Mattavelli et al., 1983). Both sediments (i.e., 0.5 to 1.0% C_{org}; mainly terrestrial kerogen with 13–14% marine phytoplankton; vitrinite reflectance less than 0.5%) are turbidites and pelagites deposited on active continental margins.

Migration Phenomena of the C_{15+} Hydrocarbons(?)

In some cases, the extract yields of the Nankai Trough sediments (Table 3) are extremely high compared to the extract yields of different kerogen types at a similar maturation level to other DSDP sediments (von der Dick et al., 1983; Rullkötter, Mukhopadhyay, and Welte, 1984; Rullkötter, Mukhopadhyay, Schaefer, et al., 1984). For example, in immature black shales, the extract yield fluctuates between 7.3 and 24.1 mg/g C_{org} and the total hydrocarbons vary between 4.7 and 36.0%. In comparison, the extract yields at Site 582 fluctuate between 11.8 and 116.7 mg/g C_{org} and at Site 583 between 10.1 and 105.1 mg/g C_{org}. Total hydrocarbon concentrations at Site 582 range between 2.3 and 20.0% (part may be mudline contamination) and between 9.5 and 62.7% at Site 583. Taking into account the organic carbon content, kerogen type, and maturation level, these sediments show anomalously high extract yields at both sites and

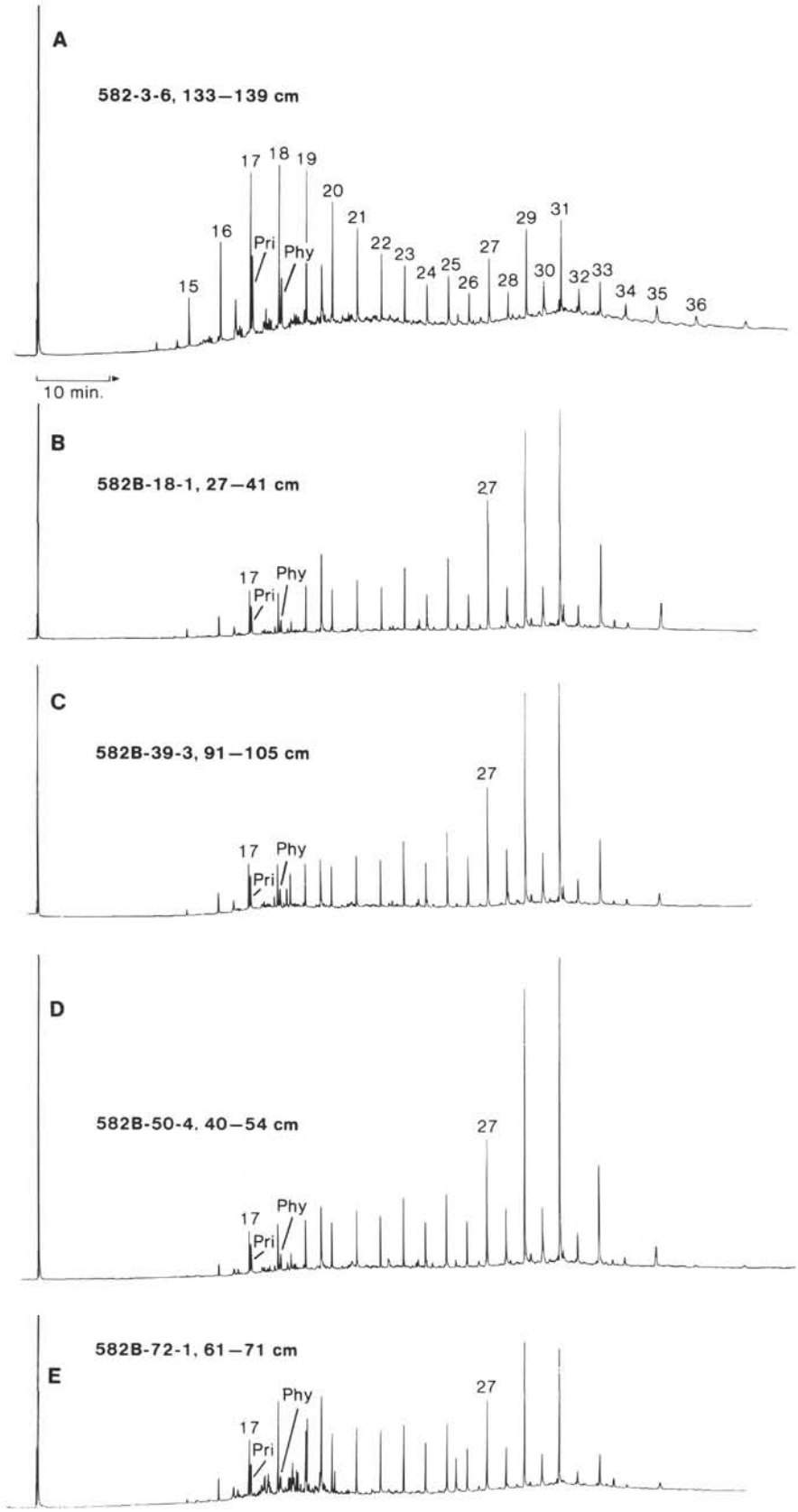

Figure 6. Capillary gas chromatograms of the nonaromatic hydrocarbon fraction of selected sediment samples from Site 582; *n*-alkanes indicated by their carbon number (Fig. 6A). Pri = Pristane, Phy = Phytane. A–E for reference to text.

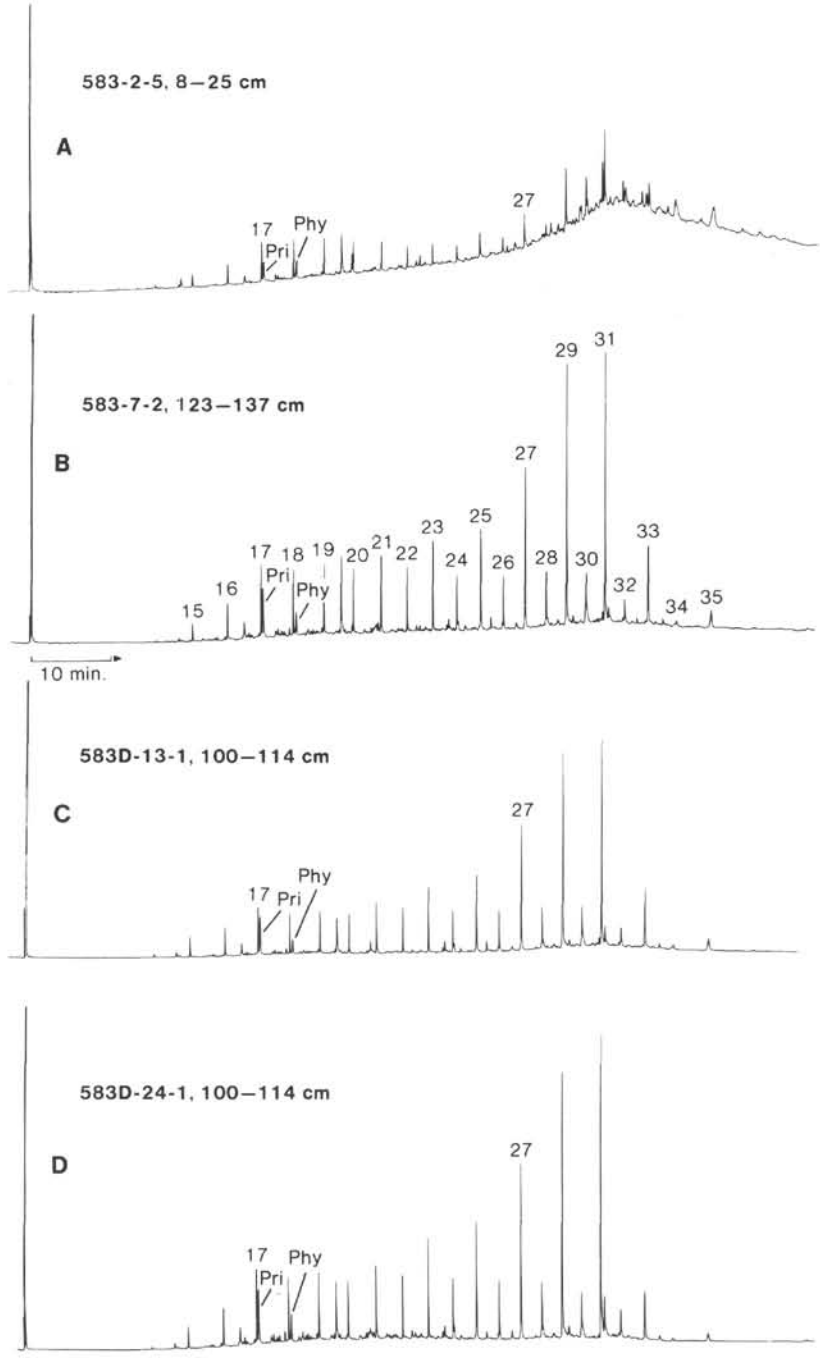

Figure 7. Capillary gas chromatograms of the nonaromatic hydrocarbon fraction of selected sediment samples from Site 583; *n*-alkanes indicated by their carbon number (Fig. 7B): Pri = Pristane; Phy = Phytane. A–D for reference to text.

unusually high relative hydrocarbon contents at Site 583. In most cases, the sediments with high extract yields are associated with sandy layers, fracture zones, or sections of poor core recovery (supposedly because of the presence of coarse sands; Leg 87 Scientific Party, 1983; site chapters, Sites 582 and 583, this volume). Porosity is greatly reduced from 65 to 45% or even less in the upper trench-fill unit at Site 582 (Karig et al., 1983). The geochemical data indicate an early generation of polar compounds and perhaps redistribution of low molecular weight organic components. These occurrences may be related to the high gas content in the sediments or water movement induced by subduction tectonics.

SUMMARY

The most important results of the organic geochemical investigation of sediment samples from DSDP Sites 582 and 583 in the Nankai Trough can be summarized as follows:

1. The organic carbon contents at both sites are fairly uniform (0.35–0.77%), with no major difference be-

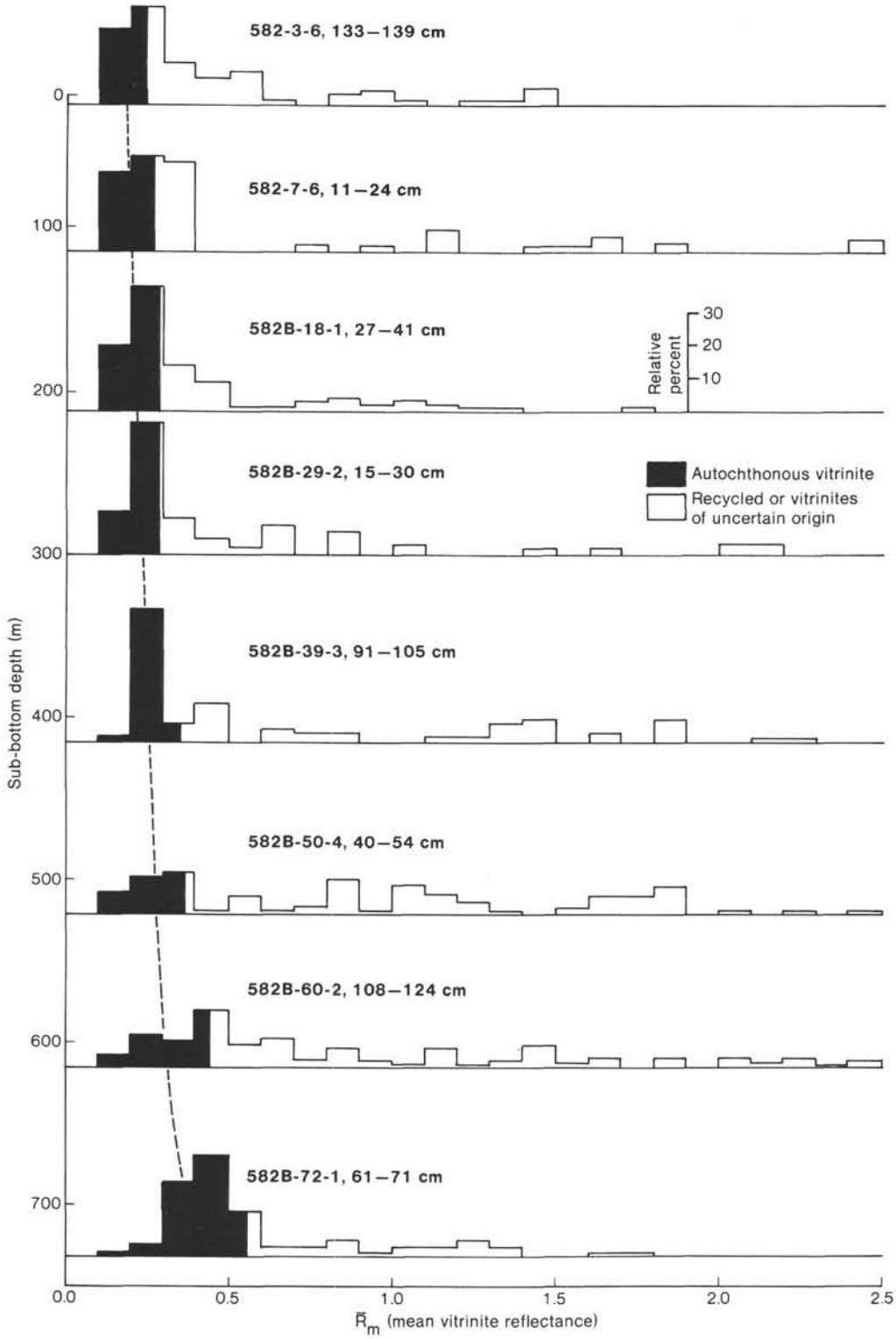

Figure 8. Vitrinite reflectance histogram (relative percent) against depth (m) for the Site 582 sediments. Dashed line indicates the change in reflectance with sub-bottom depth.

tween trench-fill turbidites and hemipelagic sediments. The moderate organic carbon contents, despite high sedimentation rates, are a consequence of the combined effects of low autochthonous bioproductivity, deposition in a deep oxic environment, and dilution by an abundance of lithogenic material.

2. The organic matter is characterized as mainly type III kerogen with a slight tendency to a mixed type II-III. Organic petrography revealed a mixture of three maceral types from different sources:

a. Fresh, green fluorescent alginite of aquatic origin was probably transported by the turbidites from the shelf

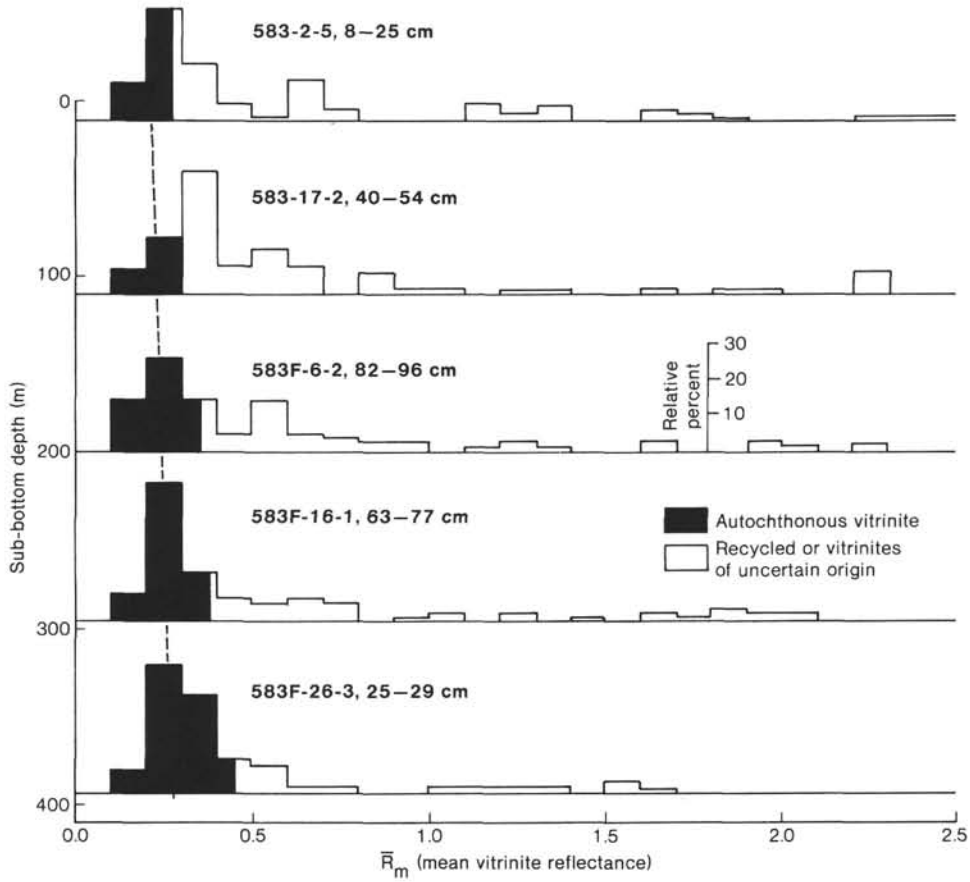

Figure 9. Vitrinite reflectance histogram (relative percent) against depth (m) for the Site 583 sediments. Autochthonous and allochthonous vitrinites as defined from the microscopic features show different markings. Dashed line indicates the change in reflectance with sub-bottom depth.

edge. The good preservation of these alginites is unusual for this water depth (about 5000 m).

b. Mainly gelified huminites mixed with terrestrial particulate liptinite and low-reflectance sclerotinite were derived from partly gelified peat or brown coal. The reasonably good preservation indicates an origin from a nearby coastal swamp environment.

c. High-reflectance inertodetrinite, vitrinite (above 1% $\bar{R}_m$), bimacerite, and micrinitized phytoclasts were derived from eroded older continental sediments; final deposition occurred distally after distal transport.

3. Several geochemical parameters provide evidence that the organic matter in the sediments is immature with respect to hydrocarbon generation; in particular, the primary organic matter indicates a mild thermal history. This immaturity is in contrast to anomalously high extract yields at both sites and in addition, high hydrocarbon proportions in the extracts at Site 583. The geochemical data indicate early generation of polar material, which usually is common only in carbonates but not in clastic sediments such as those found in the Nankai Trough, and perhaps migrational transport of low-molecular-weight organic components; this process may be related to the high gas content in the sediments and/or water movement in the unconsolidated sediments induced by subduction tectonics.

4. Carbon isotope data and chemical composition of the gases in the Nankai Trough indicate an origin from bacterial degradation of organic matter. Microscopically, a few bacterially degraded maceral components were detected. Thus, the hydrocarbon gas may either come from deeper strata (an alleged gas hydrate zone that exists in a dispersed form) or be formed by microorganisms living mainly on the (dissolved) low-molecular-weight organic components.

ACKNOWLEDGMENTS

We are indebted to Dr. M. Radke for the bitumen extraction and liquid chromatography data, Dr. P. J. Müller for organic carbon and Rock-Eval pyrolysis data, and Dr. M. Schoell, Bundesanstalt für Geowissenschaften und Rohstoffe, Hannover, for the isotopic analysis. We gratefully acknowledge careful reviews of the manuscript by Drs. Phillip A. Meyers (University of Michigan, Ann Arbor, Michigan), H. W. Hagemann (Rheinisch-Westfälische Technische Hochschule Aachen, Federal Republic of Germany), P. J. Müller (ICH-5, Kernforschungsanlage Jülich), and an anonymous reviewer. Technical assistance by Mr. W. Benders, Mrs. M. Derichs, Miss A. Fischer, Mrs. B. Kammer, Miss A. Richter, Mr. J. Schnitzler, and Miss K. Sellinghoff is gratefully acknowledged. We also thank Mrs. B. Schmitz for typing the manuscript. P.K.M. is grateful to the Deutsche Forschungsgemeinschaft (DFG), Bonn, and the National Science Foundation, Washington, for the chance to participate in DSDP Leg 87A as shipboard organic geochemist. We acknowledge the financial support of DFG (Bonn) Grant No. We 346/25.

REFERENCES

Bostick, N. H., Cashman, S. M., McCulloh, T. H., and Waddell, C. T., 1979. Gradients of vitrinite reflectance and present temperature in the Los Angeles and Ventura basins, California. *In* Oltz, D. F. (Ed.), *Low Temperature Metamorphism of Kerogen and Clay Minerals. The Pacific Section:* Los Angeles, California (Soc. Econ. Paleontol. Mineral.), pp. 65–96.

Dow, W. G., 1978. Petroleum source beds on continental slopes and rises. *Am. Assoc. Pet. Geol. Bull.*, 62:1584–1606.

Espitalié, J., Laporte, J. L., Madec, M., Marquis, F., Leplat, P., Paulet, J., and Boutefeu, A., 1977. Méthode rapide de caractérisation des roches-mères, de leur potentiel pétrolier et de leur degré d'évolution. *Rev. Inst. Fr. Pet.*, 32:23–42.

Espitalié, J., Madec, M., and Tissot, B., 1980. Role of mineral matrix in kerogen pyrolysis: influence on petroleum generation and migration. *Am. Assoc. Pet. Geol. Bull.*, 64:59–66.

Gormly, J., and Mukhopadhyay, P. K., 1983. Hydrocarbon potential of kerogen types by pyrolysis-gas chromatography. *In* Bjorøy, M., Albrecht, P., Cornford, C., de Groot, K., Eglinton, G., Galimov, E., Leythaeuser, D., Pelet, R., Rullkötter, J., and Speers, G. (Eds.), *Advances in Organic Geochemistry—1981:* Chichester (Wiley), pp. 597–606.

Karig, D. E., Kagami, H., and DSDP Leg 87 Scientific Party, 1983. Varied responses to subduction in Nankai Trough and Japan Trench forearcs. *Nature*, 304(5922):148–151.

Leg 87 Scientific Party, 1983. Leg 87 drills off Honshu and southwest Japan. *Geotimes*, 28(1):15–18.

Mattavelli, L., Ricchinto, T., Grignani, D., and Schoell, M., 1983. Geochemistry and habitat of natural gases in the Po Basin/Northern Italy. *Am. Assoc. Pet. Geol. Bull.*, 67(12):2239–2254.

Mukhopadhyay, P. K., Hagemann, H. W., and Gormly, J. R., 1985. Characterization of kerogens as seen under the aspects of maturation and hydrocarbon generation. *Erdoel Kohle Erdgas Petrochem.*, 38:7–18.

Mukhopadhyay, P. K., Rullkötter, J., and Welte, D. H., 1983. Facies and diagenesis of organic matter in sediments from the Brazil Basin and the Rio Grande Rise, Deep Sea Drilling Project Leg 72. *In* Barker, P. F., Carlson, R. L., Johnson, D. A., et al., *Init. Repts. DSDP*, 72: Washington (U.S. Govt. Printing Office), 821–828.

Peters, K. E., and Simoneit, B. R. T., 1982. Rock-Eval pyrolysis of Quaternary sediments from Leg 64, Sites 479 and 480, Gulf of California. *In* Curray, J. R., Moore, D. G., et al., *Init. Repts. DSDP*, 64, Pt. 2: Washington (U.S. Govt. Printing Office), 925–931.

Radke, M., Sittardt, H. G., and Welte, D. H., 1978. Removal of soluble organic matter from rock samples with a flow-through extraction cell. *Anal. Chem.*, 50:663–665.

Radke, M., Willsch, H., and Welte, D. H., 1980. Preparative hydrocarbon group type determination by automated medium pressure liquid chromatography. *Anal. Chem.*, 52:406–411.

Rullkötter, J., Cornford, C., Flekken, P., and Welte, D. H., 1980. Organic geochemistry of sediments cored during Deep Sea Drilling Project Legs 56 and 57, Japan Trench: organic petrography and extractable hydrocarbons. *In* Scientific Party, *Init. Repts. DSDP*, 56, 57, Pt. 2: Washington (U.S. Govt. Printing Office), 1291–1304.

Rullkötter, J., Flekken, P., and Welte, D. H., 1980. Organic petrography and extractable hydrocarbons of sediments from the northern Phillippine Sea, Deep Sea Drilling Project Leg 58. *In* Klein, G. de V., Kobayashi, K., et al., *Init. Repts. DSDP*, 58: Washington (U.S. Govt. Printing Office), 755–762.

Rullkötter, J., Mukhopadhyay, P. K., Schaefer, R. G., and Welte, D. H., 1984. Geochemistry and petrography of organic matter in sediments from DSDP Sites 545 and 547, Mazagan Escarpment. *In* Hinz, K., Winterer, E. L., et al., *Init. Repts. DSDP*, 79: Washington (U.S. Govt. Printing Office), 775–806.

Rullkötter, J., Mukhopadhyay, P. K., and Welte, D. H., 1984. Geochemistry and petrography of organic matter in sediments from Hole 530A, Angola Basin, and Hole 532, Walvis Ridge, Deep Sea Drilling Project. *In* Hay, W. W., Sibuet, J.-C., et al., *Init. Repts. DSDP*, 75: Washington (U.S. Govt. Printing Office), 1069–1088.

Schoell, M., 1982. Stable isotopic analysis of interstitial gases in Quaternary sediments from the Gulf of California. *In* Curray, J. R., Moore, D. G., et al., *Init. Repts. DSDP*, 64, Pt. 2: Washington (U.S. Govt. Printing Office), 815–817.

_____, 1983. Genetic characterization of natural gases. *Am. Assoc. Pet. Geol. Bull.*, 67(12):2225–2238.

Stach, E., Mackowsky, M. T., Teichmüller, M., Taylor, G. H., Chandra, D., and Teichmüller, R., 1982. *Coal petrology:* Berlin, Stuttgart (Gebrüder Bornträger).

Teichmüller, M., and Durand, B., 1983. Fluorescence microscopical rank studies on liptinites and vitrinites in peat and coals, and comparison with results of the Rock-Eval pyrolysis. *Int. J. Coal Geol.*, 2:197–230.

Teichmüller, M., and Ottenjahn, K., 1977. Art und Diagenese von Liptiniten und lipoiden Stoffen in einem Erdölmuttergestein aufgrund fluoreszenzmikroskopischer Untersuchungen. *Erdoel Kohle*, 30:387–398.

Tissot, B., Deroo, G., and Herbin, T. P., 1979. Organic matter in Cretaceous sediments of the North Atlantic: Contribution to sedimentology and paleogeography. *In* Talwani, M., Hay, W., and Ryan, W. B. F. (Eds.), *Deep drilling results in the Atlantic Ocean: continental margins and paleoenvironment:* Washington (Am. Geophys. Union) Maurice Ewing Series 3, 362–374.

von der Dick, H., Rullkötter, J., and Welte, D. H., 1983. Content, type, and thermal evolution of organic matter in sediments from the eastern Falkland Plateau, Deep Sea Drilling Project, Leg 71. *In* Ludwig, W. J., Krasheninnikov, V. A., et al., *Init. Repts. DSDP*, 71, Pt. 2: Washington (U.S. Govt. Printing Office), 1015–1031.

Yamano, M., 1982. New method of heat flow estimation from gas hydrate and its application to the Nankai trough area. [Master's thesis.]. University of Tokyo, Tokyo.

Date of Initial Receipt: 6 February 1984
Date of Acceptance: 18 June 1984